PSFC/JA-10-2

Trajectories, orbit squeezing, and residual zonal flow in a tokamak pedestal

Matt Landreman and Peter J. Catto

February 2010

Plasma Science and Fusion Center
Massachusetts Institute of Technology
167 Albany Street
Cambridge, MA 02139 USA

This work was supported by the U.S. Department of Energy, Grant No. DE-FG02-91ER-54109 . Reproduction, translation, publication, use and disposal, in whole or in part, by or for the United States government is permitted.
Submitted to Plasma Physics & Controlled Fusion 2010

Trajectories, orbit squeezing, and residual zonal flow in a tokamak pedestal

Matt Landreman and Peter J Catto

Massachusetts Institute of Technology, Plasma Science and Fusion Center

167 Albany St., Cambridge, MA 02139, USA

landrema@mit.edu

Abstract

Particle orbits and the Rosenbluth-Hinton residual zonal flow are evaluated for the case of a strong equilibrium radial electric field $E_r = -(d\phi / d\psi)|\nabla\psi|$ as observed in a tokamak pedestal. The ordering used is $E_r \sim B_\mathrm{p} v_\mathrm{i} / c$ where B_p is the poloidal field and v_i is the ion thermal speed. The earlier calculations of Kagan and Catto for this regime [Kagan G and Catto P J 2009 *Phys. Plasmas* **16** 056105] correctly describes the effect of a uniform $d\phi / d\psi$, but not the "orbit squeezing" effects associated with electric field shear $d^2\phi / d\psi^2$ [Kagan G and Catto P J 2009 *Phys. Plasmas* **16** 099902]. The present work gives the corrected dependence on electric field shear for a quadratic equilibrium potential $\phi(\psi)$. Analytical results are given for the large-aspect-ratio limit, and a numerical approach is outlined for performing calculations at finite aspect ratio.

1. Introduction

Zonal flow is the persistent flow observed in many turbulent fluid systems, including laboratory plasmas and planetary atmospheres [1]. In tokamaks, zonal flow is the $\mathbf{E}\times\mathbf{B}$ flow associated with one component of the electrostatic potential: the component which is independent of the toroidal and poloidal angles but which varies rapidly with the radial coordinate. This potential structure is produced by nonlinear beating of drift wave modes. The radial shear of the zonal flow in turn can regulate turbulence and its associated anomalous transport. The amplitude of the zonal flow is determined by a competition between driving and damping processes.

In references [2-3], Rosenbluth and Hinton quantify these damping processes by introducing the concept of *residual* zonal flow. In this model, the nonlinear drive for zonal flow in the kinetic equation is effectively replaced by a delta function in time. On the timescale of ion bounce motion, the ions' radial drift partially shields the initial potential perturbation $\delta\phi(t=0)$. The residual zonal flow is then defined as the ratio $\delta\phi(t\to\infty)/\delta\phi(t=0)$. Later calculations have included the effects of collisions [3, 4], plasma shaping [5, 6], and short radial wavelengths [7, 8]. The calculation has also been done in nonaxisymmetric geometry [9, 10]. Analytical expressions for the residual, obtained using a large-aspect-ratio approximation, can be used to validate gyrokinetic and gyrofluid turbulence codes. The residual also gives insight into the zonal flow amplitude which can be expected in the presence of turbulence.

Zonal flow is thought to underlie the transport suppression associated with the H-mode pedestal. It is observed in experiments that density scale-lengths in the pedestal can be comparable to the poloidal ion gyroradius $\rho_{\mathrm{p}} = \rho_{\mathrm{i}} B / B_{\mathrm{p}}$. Here, $\rho_{\mathrm{i}} = v_{\mathrm{i}} / \Omega$, $v_{\mathrm{i}} = \sqrt{2T/M}$ is the ion thermal speed, $\Omega = ZeB/Mc$ is the ion gyrofrequency, and B_{p} is the poloidal magnetic field. Assuming the toroidal flow is subsonic and the poloidal flow is small compared to $v_{\mathrm{i}} B_{\mathrm{p}} / B$, then ion radial momentum balance is roughly given by $dp_{\mathrm{i}}/dr \approx ZenE_r$ where E_r is the radial electric field. It follows that

$$E_r \sim B_{\mathrm{p}} v_{\mathrm{i}} / c \,. \tag{1}$$

Radial electric fields of this magnitude are indeed measured in experiments [11].

Physical processes will be modified when the electric field is as large as (1) for several reasons. First, the boundary in phase space between trapped and passing particles is significantly shifted [12], which can be seen as follows. A particle is trapped when its total poloidal motion, the sum of parallel and drift components, is small enough that the mirror force can stop the particle before it reaches the inboard midplane. For $E_r \sim B_{\mathrm{p}} v_{\mathrm{i}} / c$, this total poloidal motion receives contributions of comparable magnitude from the parallel motion and the $\mathbf{E}\times\mathbf{B}$ drift. It is therefore not particles of small $v_{||}$ which are trapped, but rather particles for which the two contributions nearly cancel. This statement can be expressed mathematically by noting that the net poloidal motion is given by

$$\dot{\theta} \approx \left(v_{\|}\mathbf{b} + \mathbf{v}_{\mathrm{E\times B}} \right) \cdot \nabla\theta = \left(v_{\|} + u \right) \mathbf{b} \cdot \nabla\theta \tag{2}$$

where θ is a poloidal angle-like coordinate, $\mathbf{b} = \mathbf{B} / B$,

$$u = \frac{cI}{B} \frac{d\phi}{d\psi}, \tag{3}$$

I is the toroidal magnetic field times R, and ϕ is the electrostatic potential. Since trapped particles are the particles for which $\dot{\theta}$ can vanish, we therefore expect the particles trapped about the equatorial plane to be those localized in phase space near $v_{\|} \approx -u$. This localization will be proven rigorously in section 2.

A second reason to expect physical processes to change in the strong electric field regime (1) is provided by kinetic theory. The $\left(\mathbf{v}_{\mathbf{E\times B}} \cdot \nabla\theta \right) \partial f / \partial\theta$ term must now be kept in the kinetic equation at the same order as the $\left(\mathbf{v}_{\|} \cdot \nabla\theta \right) \partial f / \partial\theta$ term. The extra term prevents the standard solution procedures from working in several calculations, including the Rosenbluth-Hinton zonal flow residual and the banana regime neoclassical fluxes. Kagan and Catto [12-14] showed this obstacle can be overcome by changing variables in the kinetic equation, replacing the radial coordinate ψ with the canonical angular momentum variable $\psi_* = \psi - Iv_{\|} / \Omega$. The Vlasov operator vanishes when acting on ψ_*, causing the coefficient of the "radial" derivative $\partial f / \partial\psi_*$ in the kinetic equation to vanish to leading order. With the number of terms in the kinetic equation thereby reduced by one, the residual and banana regime flux calculations become solvable even with the extra $\left(\mathbf{v}_{\mathbf{E\times B}} \cdot \nabla\theta \right) \partial f / \partial\theta$ term.

In reference [12], Kagan and Catto use this approach to calculate the zonal flow residual for the pedestal ordering (1). They assumed that the potential can be decomposed into an equilibrium component $\phi(\psi)$, which is constant in time on the timescale of interest, and a perturbation $\delta\phi(\psi, t)$. They further assumed that $|\nabla\phi| \gg |\nabla\delta\phi|$, and so the ordering (1) applies to $\nabla\phi$, but not to the perturbation: $\nabla\delta\phi \ll B_{\mathrm{p}} v_{\mathrm{i}} / c$. A residual value $\delta\phi(t \to \infty)$ is then calculated which reduces to the Rosenbluth-Hinton result in the limit $\phi \to 0$. This calculation in reference [12] turns out to be correct for the case of weak electric field shear ($S \to 1$), but errors were made for $S \neq 1$ [15]. These problems are each noted and corrected in the following sections. In section 2, we calculate the trajectories of particles in the presence of a strong radial electric field. Next, an integral expression for the zonal flow residual is derived in section 3. This expression contains transit averages, which are then evaluated using the trajectories found in section 2. Calculation of the residual also requires several further integrations, which are explained in section 4. The results are discussed in section 5. In section 6, it is shown how the integral expression for the residual can be evaluated numerically, without making a large-aspect-ratio expansion. We conclude in section 7, further discussing the regime in which the results are valid, noting the equations that may be of particular interest for future calculations in the pedestal regime (1), and summarizing the key results.

2. Particle Trajectories

We begin by computing the particle orbits for the case of a strong radial electric field (1). The equilibrium potential ϕ is taken to be a flux function. The value of ϕ at the location of a given particle will change during the orbit due to variation in the particle's radial coordinate. However, we ignore the radial variation of all magnetic quantities over the orbit. We therefore treat I as constant and take $B(\psi,\theta) \approx B(\theta) = B_0 / h(\theta)$. Here, B_0 is the value of B when the particle crosses the outboard midplane, so $h \le 1$.

To evaluate the transit averages which will arise in calculation of the zonal flow residual, we must express $\dot{\theta}$ from (2) in terms of only θ and constants of the motion. To achieve this goal, $v_{\|}$ is first eliminated from (2) using ψ_* conservation as follows. The canonical angular momentum is written as

$$\psi_* = \psi - \frac{McR^2}{Ze}\mathbf{v}\cdot\nabla\zeta = \psi - \frac{Iv_{\|}}{\Omega} + \frac{\mathbf{v}\times\mathbf{b}\cdot\nabla\psi}{\Omega}. \tag{4}$$

The penultimate term above is larger than the final term by B / B_{p}, so we take $\psi_* \approx \psi - Iv_{\|} / \Omega$. It follows that

$$v_{\|} = \frac{v_{\|0}}{h} + \frac{\Omega_0}{hI}\Delta\psi \tag{5}$$

where $\Delta\psi = \psi - \psi_0$. The subscript 0 again refers to values when the particle crosses the outboard midplane. This definition is unique for passing particles, which always have the same ψ when they cross through the B minimum, but not for trapped particles, for which ψ alternates between two values with each crossing. As long as all of the subscript 0 quantities for a given trajectory refer to the larger ψ crossing or all refer to the smaller ψ crossing, it is valid to choose either.

Next, the potential is Taylor-expanded to second order about ψ_0 to obtain

$$\phi \approx \phi_0 + \Delta\psi\ \phi_0' + \tfrac{1}{2}(\Delta\psi)^2 \phi_0'' \tag{6}$$

where ϕ_0, ϕ_0', and ϕ_0'' are respectively ϕ, $d\phi / d\psi$, and $d^2\phi / d\psi^2$ evaluated at the reference flux surface $\psi = \psi_0$. The validity of the Taylor approximation above will be discussed at the end of this section. From (2), (3), (5), and the derivative of (6), we obtain the following equation for the poloidal dynamics:

$$\frac{\dot{\theta}}{\mathbf{b}\cdot\nabla\theta} = v_{\|} + u = \frac{v_{\|0}}{h} + hu_0 + \frac{\Omega_0\Delta\psi}{hI}\left(1 + S_0 h^2 - h^2\right) \tag{7}$$

where

$$S_0 = 1 + \frac{cI^2\phi_0''}{B_0\Omega_0} \tag{8}$$

describes the electric field shear. Notice that if the scale-length for variation in ϕ' is comparable to ρ_{p} (as is the scale-length for variation in the density), then $S_0 - 1$ will be $O(1)$. To eliminate $\Delta\psi$ we invoke conservation of energy, which can be written using (6) as

$$\frac{v_{\|}^2}{2} + \mu B + \frac{Ze}{M}\left[(\Delta\psi)\ \phi_0' + \frac{(\Delta\psi)^2\ \phi_0''}{2}\right] = \frac{v_{\|0}^2}{2} + \mu B_0 . \tag{9}$$

After eliminating $v_{\|}$ in this relation using (5) we find

$$\begin{aligned}\Delta\psi &= \frac{I}{\Omega_0}\left(S_0 - 1 + \frac{1}{h^2}\right)^{-1} \\ &\times\left\{-\frac{v_{\|0}}{h^2} - u_0 + \sigma\sqrt{\left(\frac{v_{\|0}}{h^2} + u_0\right)^2 - \left(\frac{1}{h^2} + S_0 - 1\right)\left[v_{\|0}^2\left(\frac{1}{h^2} - 1\right) + 2\mu B_0\left(\frac{1}{h} - 1\right)\right]}\right\}\end{aligned} \tag{10}$$

where $\sigma = \pm 1$. Substituting this result into (7) we obtain

$$v_{\|} + u = \sigma\sqrt{\left(\frac{v_{\|0}}{h} + hu_0\right)^2 - \left(1 + S_0 h^2 - h^2\right)\left[v_{\|0}^2\left(\frac{1}{h^2} - 1\right) + 2\mu B_0\left(\frac{1}{h} - 1\right)\right]} . \tag{11}$$

We now consider a large-aspect-ratio model for the magnetic field well by taking $h(\theta) = 1 - 2\varepsilon\sin^2(\theta/2)$ with $\varepsilon \ll 1$. The radicand in (11) is then expanded to first order in ε, allowing $S_0 - 1$ to be order unity or smaller. Although the quantities $v_{\|0}$, u_0, and $\sqrt{\mu B_0}$ are all taken to be of order v_{i}, we must allow for the possibility that the combination $v_{\|0} + u_0$ is smaller (order $\sqrt{\varepsilon}v_{\mathrm{i}}$) or else the equation will not show particle trapping. The result of these approximations is

$$v_{\|} + u = \sigma\left|v_{\|0} + u_0\right|\sqrt{1 - \kappa^2\sin^2(\theta/2)} \tag{12}$$

with

$$\kappa^2 = \frac{4\varepsilon}{\left(v_{\|0} + u_0\right)^2}\left[(S_0 - 1)v_{\|0}^2 + u_0^2 + S_0\mu B_0\right] . \tag{13}$$

This expression corrects equation (28) in reference [12]. Note that the two expressions become equal for $S_0 = 1$. It can be seen from (12) that a particle is trapped if $\kappa^2 > 1$ and passing if $\kappa^2 < 1$. In equations (10)-(12), both signs of σ are allowed for trapped particles, while for passing particles only $\sigma = \left(v_{\|0} + u_0\right)/\left|v_{\|0} + u_0\right|$ is consistent with the requirement that $v_{\|} + u = v_{\|0} + u_0$ at $\theta = 0$. If $v_{\|0}$, u_0, and $\sqrt{\mu B_0}$ are all taken to be $O(v_{\mathrm{i}})$, then (13) shows a particle can only be trapped if $v_{\|0} + u_0$ is order $\sqrt{\varepsilon}v_{\mathrm{i}}$ or smaller. We define “freely passing” particles to be those with $v_{\|0} + u_0 \sim v_{\mathrm{i}}$ and $\kappa^2 \sim \varepsilon$, and “barely passing” particles to be those with $v_{\|0} + u_0 \sim \sqrt{\varepsilon}v_{\mathrm{i}}$ and $\kappa^2 \sim 1$.

The orbit width $w = \left|\max(\Delta\psi) - \min(\Delta\psi)\right| / \left|\nabla\psi\right|$ can be found by considering the limit of (10) for small ε, namely

$$\Delta\psi = \frac{I}{S_0\Omega_0}\left[v_{\|} + u - v_{\|0} - u_0 - 4\varepsilon v_{\|0}\sin^2(\theta/2)\right]. \tag{14}$$

The $\sin^2(\theta/2)$ term has been kept because, from (12), we see that for freely passing particles $v_{\|} + u - v_{\|0} - u_0 = (v_{\|0} + u_0)\left(\sqrt{1-\kappa^2\sin^2(\theta/2)} - 1\right) \sim \varepsilon v_{\mathrm{i}}$. It follows that $w \sim \varepsilon\rho_{\mathrm{p}}/S_0$ for these particles. For trapped and barely passing particles, $v_{\|} + u - v_{\|0} - u_0 = (v_{\|0} + u_0)\left(\sqrt{1-\kappa^2\sin^2(\theta/2)} - 1\right) \sim \sqrt{\varepsilon}v_{\mathrm{i}}$ and so $w \sim \sqrt{\varepsilon}\rho_{\mathrm{p}}/S_0$. For $S_0 \to 1$, these formulae reduce to the standard orbit widths for a weak radial electric field. If the scale-length a_ϕ for derivatives of the potential is ρ_{p}, then for all particles $w/a_\phi \le \sqrt{\varepsilon}/S_0$, so the Taylor expansion (6) is expected to be a good approximation as long as $\sqrt{\varepsilon} \ll S_0 \sim 1$. The proportionality of the orbit widths to $1/S_0$ confirms that $S_0 > 1$ describes orbit squeezing.

3. Transit averages and integral expression

We now derive an integral expression for the residual zonal flow. We begin with the gyrokinetic equation from reference [13] which uses ψ_* rather than ψ as an independent variable:

$$\frac{\partial g}{\partial t} + \dot{\theta}\frac{\partial g}{\partial \theta} = \frac{Ze}{T(\psi_*)}F\frac{\partial\delta\phi}{\partial t}, \tag{15}$$

where $g = f - \left[1 - \frac{Ze}{T(\psi_*)}\delta\phi\right]F$, f is the total distribution function, and

$$F = \eta(\psi_*)\left[\frac{M}{2\pi T(\psi_*)}\right]^{3/2}\exp\left[-\frac{ME}{T(\psi_*)}\right], \tag{16}$$

with $E = v^2/2 + Ze\phi/M$ and $T(\psi_*)$ the ion temperature evaluated at the particle location ψ_* rather than on the flux surface ψ. The function η is related to the equilibrium density $n(\psi)$ by $\eta(\psi) = n(\psi)\exp\left[Ze\phi(\psi)/T(\psi)\right]$. We consider the regime $\left|\phi/\rho_{\mathrm{p}}\right| \gtrsim |\nabla\phi| \gg |\nabla\delta\phi| \sim |k_\perp\delta\phi|$ so equation (15) is linear and $\dot{\theta}$ is given by (2). For calculation of the residual zonal flow, the potential perturbation $\delta\phi$ is taken to be a flux function. Finite gyroradius effects are not important for this derivation so we have dropped the Bessel function in (15).

We consider the dynamics of the system over a timescale τ which is long compared to the thermal bounce time $1/\dot{\theta}_{\mathrm{th}}$. We therefore expand g as a series in the small parameter $1/(\tau\dot{\theta}_{\mathrm{th}})$, writing $g = g^{(0)} + g^{(1)} + \ldots$. The leading order equation gives $\partial g^{(0)}/\partial\theta = 0$. To next order,

$$\frac{\partial g^{(0)}}{\partial t} + \dot{\theta}\frac{\partial g^{(1)}}{\partial\theta} = \frac{Ze}{T(\psi_*)}F\frac{\partial\delta\phi}{\partial t}. \tag{17}$$

The $g^{(1)}$ term can be annihilated by applying a transit average, which for any quantity A is

$$\overline{A} = \frac{\oint\left(A\,d\theta/\dot{\theta}\right)}{\oint\left(d\theta/\dot{\theta}\right)}. \tag{18}$$

As usual, $\oint(\cdot)d\theta$ indicates $\int_0^{2\pi}(\cdot)d\theta$ for regions of velocity space corresponding to passing particles, and for regions corresponding to trapped particles, $\oint(\cdot)d\theta$ means $\sum_{\sigma}\sigma\int_{\theta\min}^{\theta\max}(\cdot)d\theta$. Note that since ψ_* rather than ψ is taken as an independent variable in the gyrokinetic equation, the integrations in the transit average hold ψ_* rather than ψ fixed. Therefore, $\dot{\theta}$ in (18) is precisely that of the trajectory analyzed in section 2. Applying the transit average to (17), and noting that $\overline{g^{(0)}} = g^{(0)}$ due to the leading-order equation, we obtain

$$\frac{\partial g^{(0)}}{\partial t} = \frac{Ze}{T(\psi_*)} F \overline{\frac{\partial \delta\phi}{\partial t}}. \tag{19}$$

We take the perturbed potential to be described by an eikonal function:

$$\delta\phi(\psi,t) = \delta\hat{\phi}(t)\exp\left[iG(\psi)\right] = \delta\hat{\phi}(t)\exp\left[iG\left(\psi_* + \frac{Iv_{\|}}{\Omega}\right)\right]. \tag{20}$$

We then eliminate $v_{\|}/\Omega$ above by using equations (5) and (10) to obtain

$$\frac{Iv_{\|}}{\Omega} = \frac{I}{\Omega_0}\left[v_{\|0} + \left(S_0 - 1 + \frac{1}{h^2}\right)^{-1}\left(v_{\|} + u - \frac{v_{\|0}}{h^2} - u_0\right)\right]. \tag{21}$$

Therefore, we can Taylor expand G to obtain

$$\delta\phi \approx \delta\hat{\phi}\exp\left[iG\left(\psi_* + \frac{Iv_{\|0}}{\Omega_0}\right)\right]\exp(iP) \tag{22}$$

where

$$P = \frac{G'I}{\Omega_0}\left(S_0 - 1 + \frac{1}{h^2}\right)^{-1}\left(v_{\|} + u - \frac{v_{\|0}}{h^2} - u_0\right). \tag{23}$$

All of the quantities in (22) which are not constant during a trajectory are now contained in the P factor, so

$$\overline{\delta\phi} = \delta\hat{\phi}\exp\left[iG\left(\psi_* + \frac{Iv_{\|0}}{\Omega_0}\right)\right]\overline{e^{iP}} = \delta\phi\ e^{-iP}\overline{e^{iP}}. \tag{24}$$

Substituting this result into (19) and integrating in time from 0^- to any positive t gives

$$g^{(0)}(t) = \frac{Ze}{T(\psi_*)} F e^{-iP}\overline{e^{iP}}\delta\phi(t), \tag{25}$$

where we have taken the system state for $t<0$ to be $g=0$ and $\delta\phi = 0$.

To make further progress, we assume $|P| \ll 1$ so the exponentials in (25) can be expanded as $e^{-iP}\overline{e^{iP}} \approx 1 - iP + i\overline{P} - \left(P^2 - 2P\overline{P} + \overline{P^2}\right)/2$. To better understand the condition $|P| \ll 1$, we can use the same reasoning as in the paragraph following (14) to estimate the factor $v_{\|} + u - \left(v_{\|0}/h^2\right) - u_0$ appearing in the definition of P. We thereby find $P \sim \sqrt{\varepsilon}k_{\perp}\rho_{\mathrm{p}}/S$ for trapped and barely passing particles and $P \sim \varepsilon k_{\perp}\rho_{\mathrm{p}}/S$ for freely passing particles, where we have defined $k_{\perp} = |\nabla\psi|G'$. Consequently, $\sqrt{\varepsilon}k_{\perp}\rho_{\mathrm{p}}/S \ll 1$ is required to ensure $|P| \ll 1$ for the trapped and barely passing particles, with $\sqrt{\varepsilon} \ll 1$ needed to allow $k_{\perp}\rho_{\mathrm{p}} \gtrsim 1$.

The remainder of the zonal flow analysis follows as in reference [12], upon making the replacement $Q \to P$. The result is

$$\frac{\delta\phi(t \to \infty)}{\delta\phi(t=0)} = \frac{1}{1+\Re}, \tag{26}$$

where

$$\Re = \frac{2}{n_0 \left\langle k_\perp^2 \rho_\mathrm{i}^2 \right\rangle} \left\langle \int d^3v \; f_\mathrm{M} \left(iP - i\bar{P} + \frac{P^2 - 2P\bar{P} + \overline{P^2}}{2} \right) \right\rangle, \tag{27}$$

$$f_\mathrm{M} = \eta(\psi) \left[\frac{M}{2\pi T(\psi)} \right]^{3/2} \exp\left[-\frac{ME}{T(\psi)} \right], \tag{28}$$

and $\langle \cdot \rangle$ denotes a flux surface average. In (27), $f_\mathrm{M} = F + \ldots$ appears because the poloidal gyroradius corrections treated by standard neoclassical theory do not contribute to $\Re$.

We emphasize that the flux surface average and velocity-space integrations in (27) will be performed at constant ψ, whereas the integrals in the transit averages will instead be performed at constant ψ_*.

Using $\varepsilon \ll 1$, we approximate $P \approx P_\varepsilon$ where

$$P_\varepsilon = \frac{G'I}{S_0\Omega_0} \left[v_\| + u - v_{\|0} - u_0 - 4\varepsilon v_{\|0} \sin^2(\theta/2) \right]. \tag{29}$$

Note that this approximation is correct to the leading two orders in $\sqrt{\varepsilon}$ for both freely passing particles and for trapped and barely passing particles. We then introduce

$$Q = \frac{G'I}{S_0\Omega_0} \left(v_\| + u \right) \tag{30}$$

and

$$L = \frac{G'I}{S_0\Omega_0} \frac{4\varepsilon v_{\|0}}{\kappa^2} \left[1 - \kappa^2 \sin^2(\theta/2) \right] \tag{31}$$

and we note that $i\left(P_\varepsilon - \bar{P}_\varepsilon\right) + \left(P_\varepsilon^2 - 2P_\varepsilon \overline{P_\varepsilon} + \overline{P_\varepsilon^2}\right)/2 = i\left(L - \bar{L} + Q - \bar{Q}\right) + \left(Q^2 - 2Q\bar{Q} + \overline{Q^2}\right)/2$. Thus,

$$\Re = \frac{2}{n_0 \left\langle k_\perp^2 \rho_\mathrm{i}^2 \right\rangle} \left\langle \int d^3v \; f_\mathrm{M} \left[i\left(L - \bar{L} + Q - \bar{Q}\right) + \frac{Q^2 - 2Q\bar{Q} + \overline{Q^2}}{2} \right] \right\rangle. \tag{32}$$

This is the desired integral expression for the residual zonal flow. Note that the quantity Q defined in (30) contains an extra factor of $1/S_0$ compared to the quantity Q in reference [12].

The transit averaged quantities can be written in terms of the complete elliptic integrals of the first and second kinds:

$$K(\kappa) = \int_0^{\pi/2} \frac{d\xi}{\sqrt{1 - \kappa^2 \sin^2 \xi}}, \tag{33}$$

$$E(\kappa) = \int_0^{\pi/2} \sqrt{1 - \kappa^2 \sin^2 \xi} \; d\xi . \tag{34}$$

For passing particles, (18) yields

$$\bar{Q} = \frac{G'I}{S_0\Omega_0}\left(v_{\|0} + u_0\right)\frac{\pi}{2K(\kappa)}, \tag{35}$$

$$\overline{Q^2} = \left(\frac{G'I}{S_0\Omega_0}\right)^2 \left(v_{\|0} + u_0\right)^2 \frac{E(\kappa)}{K(\kappa)}, \tag{36}$$

and

$$\bar{L} = \frac{G'I}{S_0\Omega_0}\frac{4\varepsilon v_{\|0}}{\kappa^2}\frac{E(\kappa)}{K(\kappa)}. \tag{37}$$

For trapped particles, $\bar{Q} = 0$,

$$\overline{Q^2} = \left(\frac{G'I}{S_0\Omega_0}\right)^2 \left(v_{\|0} + u_0\right)^2 \left[\frac{\kappa^2 E\left(\kappa^{-1}\right)}{K\left(\kappa^{-1}\right)} + 1 - \kappa^2\right], \tag{38}$$

and

$$\bar{L} = \frac{G'I}{S_0\Omega_0}\frac{4\varepsilon v_{\|0}}{\kappa^2}\left[\frac{\kappa^2 E\left(\kappa^{-1}\right)}{K\left(\kappa^{-1}\right)} + 1 - \kappa^2\right]. \tag{39}$$

4. Calculation of integrals

In the original Rosenbluth-Hinton calculation, the contribution to $\Re$ from freely passing particles is higher order in the $\sqrt{\varepsilon}$ expansion compared to the contribution from the trapped and barely passing particles. We proceed by assuming this result also holds in the present strong E_r case, since the algebra becomes intractable hereafter if the contribution from freely passing particles is retained. For the rest of this section we will therefore use the orderings appropriate to trapped and barely passing particles: $v_{\|0} + u_0 = O\left(\sqrt{\varepsilon} v_{\mathrm{i}}\right)$, $v_{\|} + u = O\left(\sqrt{\varepsilon} v_{\mathrm{i}}\right)$, and $\kappa^2 = O(1)$. To calculate $\mathrm{Im}(\Re)$ we will need to keep the first two orders in the $\sqrt{\varepsilon}$ expansion, while for $\mathrm{Re}(\Re)$ only the leading order terms are required.

In reference [12], the d^3v integration was performed by changing to the variables κ^2 and $v_{\|0} + u_0$. However, here $v_\perp^2$ will be used as an integration variable in place of $v_{\|0} + u_0$. The reason for this change is that for $\phi'' \neq 0$ (i.e. for $S \neq 1$), the range of allowed $v_{\|0} + u_0$ becomes θ-dependent, whereas the range of $v_\perp^2$ remains simply $(0, \infty)$. The desired incremental integration volume in the new variables is then

$$d^3v = \pi\; dv_{\|}\; dv_\perp^2 = \pi \left|\left(\frac{\partial v_{\|}}{\partial \kappa^2}\right)_{\psi,\theta,v_\perp^2}\right| \sum_{\sigma=\pm 1} d\kappa^2 dv_\perp^2. \tag{40}$$

Our eventual goal is to express $\Re$ in terms of flux functions. It is therefore useful at this point to redefine u and S so they become flux functions:

$$u = \frac{cI}{B_0}\frac{d\phi}{d\psi}, \tag{41}$$

$$S = 1 + \frac{cI^2}{B_0 \Omega_0} \frac{d^2\phi}{d\psi^2} . \tag{42}$$

The differences between the new and old definitions are $O(\varepsilon)$ and therefore negligible. At the same time, the distinction between u and u_0 is important. The partial derivative in (40) holds ψ fixed rather than ψ_*, so u is considered constant. However, u_0 is *not* held constant since it contains $\phi'(\psi_0)$ and ψ_0 depends on velocity (recall that the '0' subscript denotes a quantity evaluated when a trajectory crosses the outboard midplane.) To relate u_0 to u we use (10) and $\phi'(\psi) - \phi'(\psi_0) \approx \phi''(\psi_0)\Delta\psi$ to obtain

$$u_0 = u + \left(\frac{1}{S_0} - 1\right)\left[v_{||} + u - \left(v_{||0} + u_0\right)\right] + O(\varepsilon v_{\mathrm{i}}) . \tag{43}$$

Thus, $u_0 - u_\psi \sim \sqrt{\varepsilon} v_{\mathrm{i}}$, and as stated previously, terms of this order must be kept to correctly calculate $\mathrm{Im}(\Re)$. Similarly, if ϕ'' were allowed to vary significantly over a ρ_{p} scale-length, then S and S_0 would differ by order $\sqrt{\varepsilon}$. When the S_0 factors in (32) (such as those appearing in (35)-(39)) are eliminated in favour of S factors (to perform the integrals at fixed ψ), the resulting $\sqrt{\varepsilon}$ correction terms would be large enough to affect $\mathrm{Im}(\Re)$. To avoid the complexity of these correction terms, which are proportional to the third derivative of the potential, here we take ϕ'' to be uniform. In this case we can replace S_0 by S with no error.

To evaluate the derivative in the Jacobian (40), we first use (43) and (12) to rewrite (13) as

$$\kappa^2 \approx \frac{4\varepsilon S}{\left(v_{||} + u\right)^2}\left[\frac{v_\perp^2}{2} + u^2 + 2\left(\frac{1-S}{S}\right)\left(v_{||} + u\right)u\right]\left[1 - \kappa^2 \sin^2(\theta/2)\right] \tag{44}$$

where $O\left(\varepsilon v_{\mathrm{i}}^2\right)$ terms have been neglected in the first pair of square brackets. This result is differentiated to obtain

$$\begin{aligned}\left(\frac{\partial v_{||}}{\partial \kappa^2}\right)_{\psi,\theta,v_\perp^2} &= -\frac{2\varepsilon S}{\kappa^4\left(v_{||} + u\right)}\left[\frac{v_\perp^2}{2} + u^2 + 2\left(\frac{1-S}{S}\right)\left(v_{||} + u\right)u\right] \\ &\quad \times \left[1 - \frac{4\varepsilon}{\kappa^2}\frac{(1-S)u}{\left(v_{||} + u\right)}\left(1 - \kappa^2 \sin^2\frac{\theta}{2}\right)\right]^{-1} .\end{aligned} \tag{45}$$

Expanding in $\sqrt{\varepsilon}$ leaves

$$\left|\frac{\partial v_{||}}{\partial \kappa^2}\right| = \frac{\varepsilon S\left(v_\perp^2 + 2u^2\right)}{\kappa^4\left|v_{||} + u\right|}\left[1 + \frac{4\varepsilon}{\kappa^2}\frac{(1-S)u}{\left(v_{||} + u\right)}\left(1 - \kappa^2 \sin^2\frac{\theta}{2}\right) + \frac{4}{S}\frac{(1-S)\left(v_{||} + u\right)u}{\left(v_\perp^2 + 2u^2\right)}\right]. \tag{46}$$

Next, the Maxwellian f_{M} in $\Re$ contains v^2, which can be written as

$$v^2 = v_\perp^2 + v_{||}^2 = v_\perp^2 + u^2 - 2\left(v_{||} + u\right)u + O\left(\varepsilon v_{\mathrm{i}}^2\right) . \tag{47}$$

We then expand f_{M} to obtain

$$f_{\mathrm{M}} \approx n_0 \left(\frac{M}{2\pi T}\right)^{3/2} \left[1 + 2\left(v_{\|} + u\right)\frac{u}{v_{\mathrm{i}}^2}\right] \exp\left(-\frac{v_\perp^2 + u^2}{v_{\mathrm{i}}^2}\right). \tag{48}$$

To evaluate the real part of $\Re$, we do not need to keep the $\sqrt{\varepsilon}$ correction terms in (46) and (48). Then by combining (12), (32), (35), (36), (38), (40), (46), and (48), the expression we must evaluate becomes

$$\begin{aligned} \operatorname{Re}(\Re) = {} & \frac{\varepsilon \exp\left(-u^2 / v_{\mathrm{i}}^2\right)}{2\pi^{3/2} S v_{\mathrm{i}}^3 \left\langle k_\perp^2 \rho_{\mathrm{i}}^2 \right\rangle} \left(\frac{G' I}{\Omega_0}\right)^2 \int_0^\infty dv_\perp^2 \left(v_\perp^2 + 2u^2\right) \exp\left(-\frac{v_\perp^2}{v_{\mathrm{i}}^2}\right) \int_0^\infty \frac{d\kappa^2}{\kappa^4} \int d\theta \sum_{\sigma=\pm 1} \left|v_{\|0} + u_0\right| \\ & \times \left\{ \sqrt{1 - \kappa^2 \sin^2(\theta/2)} - \frac{\pi H}{K(\kappa)} + \frac{E(\kappa) H + \left[\left(1-\kappa^2\right) K\left(\kappa^{-1}\right) + \kappa^2 E\left(\kappa^{-1}\right)\right](1-H)}{K(\kappa) \sqrt{1 - \kappa^2 \sin^2(\theta/2)}} \right\} \end{aligned} \tag{49}$$

where $H = H(1-\kappa)$ is a Heavyside function which is 1 for $\kappa < 1$ and 0 for $\kappa > 1$. The remaining factor of $\left|v_{\|0} + u_0\right|$ in the integrand is eliminated by dropping the $\sqrt{\varepsilon}$ correction in (44) and rearranging to find

$$\left|v_{\|0} + u_0\right| \approx \sqrt{\frac{2\varepsilon S}{\kappa^2}} \sqrt{v_\perp^2 + 2u^2} \, . \tag{50}$$

The θ integration in (49) is performed first, using

$$\int_{-2\sin^{-1}\left(\kappa^{-1}\right)}^{2\sin^{-1}\left(\kappa^{-1}\right)} \frac{d\theta}{\sqrt{1 - \kappa^2 \sin^2(\theta/2)}} = \frac{4}{\kappa} K\left(\kappa^{-1}\right). \tag{51}$$

The κ^2 integration can then be evaluated numerically:

$$\int_0^1 \frac{d\kappa}{\kappa^4} \left[\frac{2E(\kappa)}{\pi} - \frac{\pi}{2K(\kappa)}\right] + \frac{2}{\pi} \int_1^\infty \frac{d\kappa}{\kappa^5} \left[\left(1-\kappa^2\right) K\left(\kappa^{-1}\right) + \kappa^2 E\left(\kappa^{-1}\right)\right] = 0.193 \, . \tag{52}$$

The $v_\perp^2$ integral which remains can be expressed in terms of the error function.

Switching our consideration now to the imaginary part of $\Re$, we must keep the $\sqrt{\varepsilon}$ correction terms in (46) and (48). Since the $L - \bar{L}$ contribution to (32) is already $\sqrt{\varepsilon}$ small compared to the contribution from $Q - \bar{Q}$, we can approximate the $v_{\|0}$ in $L - \bar{L}$ by $-u$. The expression we must evaluate is therefore

$$\mathrm{Im}(\Re)=\frac{\varepsilon\exp\left(-u^2/v_{\mathrm{i}}^2\right)}{\pi^{3/2}v_{\mathrm{i}}^3\left\langle k_\perp^2\rho_{\mathrm{p}}^2\right\rangle}\frac{G'I}{\Omega_0}\int_0^\infty dv_\perp^2\left(v_\perp^2+2u^2\right)\exp\left(-\frac{v_\perp^2}{v_{\mathrm{i}}^2}\right)\int_0^\infty\frac{d\kappa^2}{\kappa^4}\int d\theta\sum_{\sigma=\pm1}$$
$$\times\left\{\frac{\sigma}{\sqrt{1-\kappa^2\sin^2(\theta/2)}}+u\left|v_{\|0}+u_0\right|\left[\frac{2}{v_{\mathrm{i}}^2}+\frac{4\varepsilon(1-S)}{\kappa^2\left(v_{\|0}+u_0\right)^2}+\frac{4(1-S)}{S\left(v_\perp^2+2u^2\right)}\right]\right\}$$
$$\times\left\{\sqrt{1-\kappa^2\sin^2(\theta/2)}-\frac{\pi H}{2K(\kappa)}\right.$$
$$\left.-\frac{4\varepsilon u}{\sigma\kappa^2\left|v_{\|0}+u_0\right|}\left[1-\kappa^2\sin^2(\theta/2)-H\frac{E(\kappa)}{K(\kappa)}-(1-H)\frac{\kappa^2E\left(\kappa^{-1}\right)+\left(1-\kappa^2\right)K\left(\kappa^{-1}\right)}{K\left(\kappa^{-1}\right)}\right]\right\}. \quad (53)$$

Both sets of curly braces in (53) enclose leading order terms followed by $\sqrt{\varepsilon}$ corrections. The product of the leading order terms is odd in σ so it vanishes when the sum over σ is performed. It is this cancellation which forces us to keep the $\sqrt{\varepsilon}$ correction terms in each set of curly braces.

As with $\mathrm{Re}(\Re)$, the θ integration in (54) is performed first. The $\sqrt{\varepsilon}$ correction in the last curly brackets of (53), which originated from the $L-\overline{L}$ in (32), vanishes in this integration. We are then left with

$$\mathrm{Im}(\Re)=\frac{2\varepsilon u\exp\left(-u^2/v_{\mathrm{i}}^2\right)}{\pi^{3/2}v_{\mathrm{i}}^4\left\langle k_\perp\rho_{\mathrm{p}}\right\rangle}\left(\frac{q}{\varepsilon}\right)^2\int_0^\infty dv_\perp^2\left(v_\perp^2+2u^2\right)\exp\left(-\frac{v_\perp^2}{v_{\mathrm{i}}^2}\right)\int_0^\infty\frac{d\kappa^2}{\kappa^4}\int d\theta\left|v_{\|0}+u_0\right|$$
$$\times\left[\frac{2}{v_{\mathrm{i}}^2}+\frac{4\varepsilon(1-S)}{\kappa^2\left(v_{\|0}+u_0\right)^2}+\frac{4(1-S)}{S\left(v_\perp^2+2u^2\right)}\right]\left[\sqrt{1-\kappa^2\sin^2(\theta/2)}-\frac{\pi H}{2K(\kappa)}\right] \quad (54)$$

where $q\approx\varepsilon B/B_{\mathrm{p}}$ is the safety factor. Following the θ integration and the application of (50), the κ integral becomes identical to (52).

5. Analytical results

Upon performing the integrations, the residual zonal flow can be expressed as

$$\Re=\Re_{\mathrm{RH}}\left[\frac{\Upsilon(U)}{\sqrt{S}}+i\frac{\Lambda(U,S)}{\left\langle k_\perp\rho_{\mathrm{p}}\right\rangle}\right] \quad (55)$$

where $\Re_{\mathrm{RH}}=1.64q^2/\sqrt{\varepsilon}$ is the Rosenbluth-Hinton (weak E_r) result, $U=u/v_{\mathrm{i}}$,

$$\Upsilon(U)=\frac{4e^{-U^2}}{3\sqrt{\pi}}\int_0^\infty e^{-y}\left(y+2U^2\right)^{3/2}dy$$
$$=|U|e^{-U^2}\sqrt{\frac{2}{\pi}}\left(2+\frac{8}{3}U^2\right)+e^{U^2}\left[1-\mathrm{erf}\left(\sqrt{2}|U|\right)\right] \quad (56)$$

gives the real part of $\Re$, and

$$\begin{aligned}\Lambda(U,\,S) &= \frac{2U}{\sqrt{S}}\left[S\Upsilon(U)+(1-S)\frac{4e^{-U^2}}{\sqrt{\pi}}\int_0^\infty e^{-y}\sqrt{y+2U^2}\,dy\right] \\ &= \frac{2U}{\sqrt{S}}\left[S\Upsilon(U)+2(1-S)\left\{2|U|e^{-U^2}\sqrt{\frac{2}{\pi}}+e^{U^2}\left[1-\operatorname{erf}\left(\sqrt{2}|U|\right)\right]\right\}\right]\end{aligned} \tag{57}$$

describes the imaginary part. The above two functions are plotted in figure 1. The function Υ is even in U, while Λ is odd in U.

For $S=1$, the U dependence of the residual zonal flow (55) is identical to that given in reference [12]. Although the quantitative results differ for $S\neq 1$, the qualitative results discussed in reference [12] remain true. The electric field shear $d^2\phi/d\psi^2$ affects $\Re$ only algebraically (through S), whereas the field magnitude $d\phi/d\psi$ affects $\Re$ exponentially through U. For $|U|\gtrsim 1$, the trapped-passing boundary is shifted to the exponentially decaying part of the Maxwellian. Since trapped and barely passing particles provide the dominant contribution to $\Re$, both Υ and Λ (and therefore $\Re$) decay exponentially for large $|U|$. Thus, when the equilibrium electric field is strong as in a pedestal, collisionless damping of zonal flows can be suppressed. This suppression can in principle result in a positive feedback cycle, as turbulent transport is reduced, the density gradient steepens, and therefore E_r is reinforced.

6. Numerical integration

For a specified magnetic field, the integrals in (27) can also be evaluated numerically without making use of the $\sqrt{\varepsilon}\ll 1$ approximation. For this calculation we use a model magnetic field $B=B_0/h$ where $h=(1+\varepsilon\cos\theta)/(1+\varepsilon)$, ε is now taken to be finite, and $\mathbf{b}\cdot\nabla\theta=$ uniform. More sophisticated $h(\theta)$ and $\mathbf{b}\cdot\nabla\theta$ functions could also be used. The transit averages are evaluated using (11) without further approximation. As in the analytical calculation, the equilibrium potential $\phi(\psi)$ is taken to be a perfectly quadratic function of ψ so that S_0 is equal to the S defined in (42). The transit averages calculated from (11) are functions of $v_{\|0}$ and u_0, so we must calculate $v_{\|0}$ and u_0 in terms of $\mathbf{v}$ and θ to carry out the $\int d^3v$ and $\int d\theta$ integrals. To this end, we perform the same analysis as in equations (5)-(11), but this time expanding the potential about ψ rather than ψ_0, and eliminating $v_{\|0}$ instead of $v_{\|}$. The result is

$$u_0=u+\frac{(1-S)\left(hv_{\|}+u\right)}{S}\left\{1-\sqrt{1+\frac{S}{\left(hv_{\|}+u\right)^2}\left[v_{\|}^2\left(1-h^2\right)+2\mu B_0\left(\frac{1}{h}-1\right)\right]}\right\} \tag{58}$$

and

$$v_{\|0}=hv_{\|}-\frac{hv_{\|}+u}{S}\left\{1-\sqrt{1+\frac{S}{\left(hv_{\|}+u\right)^2}\left[v_{\|}^2\left(1-h^2\right)+2\mu B_0\left(\frac{1}{h}-1\right)\right]}\right\} \tag{59}$$

with u and S defined by (41)-(42). For trapped particles there are actually two valid $\left(v_{\|0}, u_0\right)$ pairs for each $\left(\theta, \mathbf{v}\right)$, and there is an associated choice in the sign of the square roots above. However, the choice used in (58)-(59) ensures $v_{\|0} = v_{\|}$ at $\theta = 0$ for passing particles, so (58)-(59) are valid for all particles and are therefore convenient forms.

The transit average is defined differently for trapped and passing particles, as described following (18). Therefore, for each $\left(\theta, \mathbf{v}\right)$, to determine if the associated trajectory is passing or trapped, the sign of the radicand of (11) is evaluated at $h = h_{\min} = \left(1-\varepsilon\right)/\left(1+\varepsilon\right)$. A positive (negative) sign indicates passing (trapped). Notice that unlike the analytical calculation described in section 4, the numerical calculation fully accounts for freely passing particles.

Numerical noise was found to be reduced when

$$x = \frac{4\varepsilon\mu B_0}{v^2 - 2\mu B_0} \tag{60}$$

and v / v_{i} were chosen as the variables for the $\int d^3 v$ integration. A sum is performed over both signs of $v_{\|}$, with $\sigma = \mathrm{sgn}\left(v_{\|} + hu\right)$ calculated for each value of $v_{\|}$. Numerical noise was also reduced when the $\mathrm{sgn}\left(v_{\|}\right)$ sum and θ integral are performed before the x and v integration. Calculation of $\Re$ for any given U and S takes 5-60 minutes using the *quad* routine in MATLAB on a typical desktop PC.

Figure 2 shows values of $\Re$ calculated using the preceding procedure. For comparison, the approximate analytical form in (55) is plotted on the same graph.

7. Discussion

The numerical results converge to the analytical form (55) as $\varepsilon \to 0$ as desired, as shown in figure 2. For the analytical expression to be a good approximation to the finite ε value, ε must be smaller than values relevant to experiment. However, the analytical form is still valuable for validating turbulence codes, since ε in these codes can be made arbitrarily small. Also, qualitative features of the analytical result can be expected to persist at finite aspect ratio. For example, we can generally expect $\Re$ to have an imaginary part which scales as $\mathrm{Im}\left(\Re\right) / \mathrm{Re}\left(\Re\right) \sim \left(k_\perp \rho_{\mathrm{p}}\right)^{-1}$.

The key reason for the difference in figure 2 between the analytical and numerical values of $\Re$ is the following. We can write $\Re = \sum_j \Re_j$, where $j = \mathrm{t}$ for trapped and barely passing particles, $j = \mathrm{p}$ for freely passing particles, and $\Re_j$ is the contribution to $\Re$ from particles of type j. We can also write $\Re_j = f_j \alpha_j$, where f_{p} is the fraction of the distribution which is freely passing, f_{t} is the fraction of particles which are trapped or barely passing, and α_j reflects the contribution to $\Re$ per particle. Multiplying the conventional (weak E_r) trapped fraction $\sqrt{\varepsilon}$ by the exponentially small fraction of particles with $v_{\|} \approx -u$, we estimate $f_{\mathrm{t}} \sim \sqrt{\varepsilon} \exp\left(-U^2\right)$. Notice f_{p} is of order unity with no strong U dependence. Figure 2 confirms that $\Re \to \Re_{\mathrm{t}}$ as $\sqrt{\varepsilon} \to 0$, so $\Re_{\mathrm{p}}$ must be small in $\sqrt{\varepsilon}$ compared to $\Re_{\mathrm{t}}$, and we therefore expect $\alpha_{\mathrm{p}} / \alpha_{\mathrm{t}} \sim \varepsilon$. The ratio $\alpha_{\mathrm{p}} / \alpha_{\mathrm{t}}$ will not have exponential U dependence, since the contributions to $\Re$ *per particle* are independent of the shape of the distribution function. Thus, $\Re_{\mathrm{t}} / \Re_{\mathrm{p}} \sim \exp\left(-U^2\right) / \sqrt{\varepsilon}$. The analytical result (55) therefore requires $\sqrt{\varepsilon} \ll \exp\left(-U^2\right)$. When this inequality is violated, freely passing particles provide a significant contribution to the residual zonal flow.

Another important point should be made concerning the range of zonal flow wavelengths ($k_\perp$) for which (55) and the numerical method of section 6 are valid. In tokamak experiments, the radial electric field is only observed to be as large as (1) over a region of radial width $\sim \rho_{\mathrm{p}}$. In this case, the assumption of a quadratic potential $\phi(\psi)$ used herein will be reasonable for $k_\perp \rho_{\mathrm{p}} > 1$. In turbulence codes, a quadratic $\phi(\psi)$ can be imposed over a range of ψ corresponding to many ρ_{p}. In this scenario, (55) and the numerical method of section 6 would be valid even if $k_\perp \rho_{\mathrm{p}} \sim 1$.

Many of the results as well as the methods used here can be used to calculate other quantities in the strong E_r pedestal regime (1), such as the neoclassical ion heat flux and ion parallel flow [14]. In particular, equation (13) gives the trapping parameter κ^2 in this regime, correcting the κ^2 in reference [12] when orbit squeezing is present. Moreover, equations (11), (14), (21), (43), (46), (58), and (59) provide useful relations involving the constants of the motion u_0, $v_{\|0}$, and κ^2.

To summarize, we have derived the effect of orbit squeezing on the trapped-passing boundary and on the residual zonal flow in the strong E_r pedestal regime (1). The trapped-passing boundary is shifted in $v_\|$ by an amount proportional to E_r, so the trapped fraction becomes exponentially small. Consequently, the magnitude of E_r has an exponential effect on the residual zonal flow, whereas the orbit squeezing parameter S has an algebraic effect. When E_r exceeds $\sim B_{\mathrm{p}} v_{\mathrm{i}} / c$, collisionless damping of zonal flow is suppressed. A positive feedback loop therefore continues to exist [12, 13], in which a strong density gradient will cause a strengthening of zonal flow, suppressing turbulent transport, and thereby reinforcing the density gradient.

Acknowledgments

The authors thank Grigory Kagan for many useful conversations.

This research was supported by the United States Department of Energy under grant DE-FG02-91ER-54109.

References

[1] Diamond P H, Itoh S-I, Itoh K and Hahm T S 2005 *Plasma Phys. Controlled Fusion* **47** R35

[2] Rosenbluth M N and Hinton F L 1998 *Phys. Rev. Lett.* **80** 724

[3] Hinton F L and Rosenbluth M N 1999 *Plasma Phys. Controlled Fusion* **41** A653

[4] Xiao Y, Catto P J and Molvig K 2007 *Phys. Plasmas* **14** 032302

[5] Xiao Y and Catto P J 2006 *Phys. Plasmas* **13** 082307

[6] Shi B 2007 *Plasma Phys. Controlled Fusion* **49** 2019

[7] Xiao Y and Catto P J 2006 *Phys. Plasmas* **13** 102311

[8] Xiao Y, Catto P J and Dorland W 2007 *Phys. Plasmas* **14** 055910

[9] Sugama H and Watanabe T-H 2005 *Phys. Rev. Lett.* **94** 115001

[10] Mishchenko A, Helander P and Könies A 2008 *Phys. Plasmas* **15** 072309

[11] McDermott R M *et al* 2009 *Phys. Plasmas* **16** 056103

[12] Kagan G and Catto P J 2009 *Phys. Plasmas* **16** 056105

[13] Kagan G and Catto P J 2008 *Plasma Phys. Controlled Fusion* **50** 085010

[14] Kagan G and Catto P J 2009 *Plasma Phys. Controlled Fusion* submitted

[15] Kagan G and Catto P J 2009 *Phys. Plasmas* **16** 099902

Figure Captions

1. (Colour online) The numerical functions Υ and Λ appearing in the (a) real and (b) imaginary parts of $\Re$ respectively. In (b), the thick contour indicates zero, and other contours indicate multiples of 0.5.

2. (Colour online) Scaled (a) real and (b) imaginary parts of $\Re$ for $S = 3$. The scale factors are $C_{\mathrm{R}} = \left(G' I v_{\mathrm{i}} / \Omega_0\right)^2 \left\langle k_\perp^2 \rho_{\mathrm{i}}^2 \right\rangle^{-1} \varepsilon^{3/2} \approx q^2 \varepsilon^{-1/2}$ and $C_{\mathrm{I}} = G' I v_{\mathrm{i}} \Omega_0^{-1} \left\langle k_\perp^2 \rho_{\mathrm{i}}^2 \right\rangle^{-1} \varepsilon^{3/2} \approx q^2 \varepsilon^{-1/2} \left(k_\perp \rho_{\mathrm{p}}\right)^{-1}$.

Figure 1

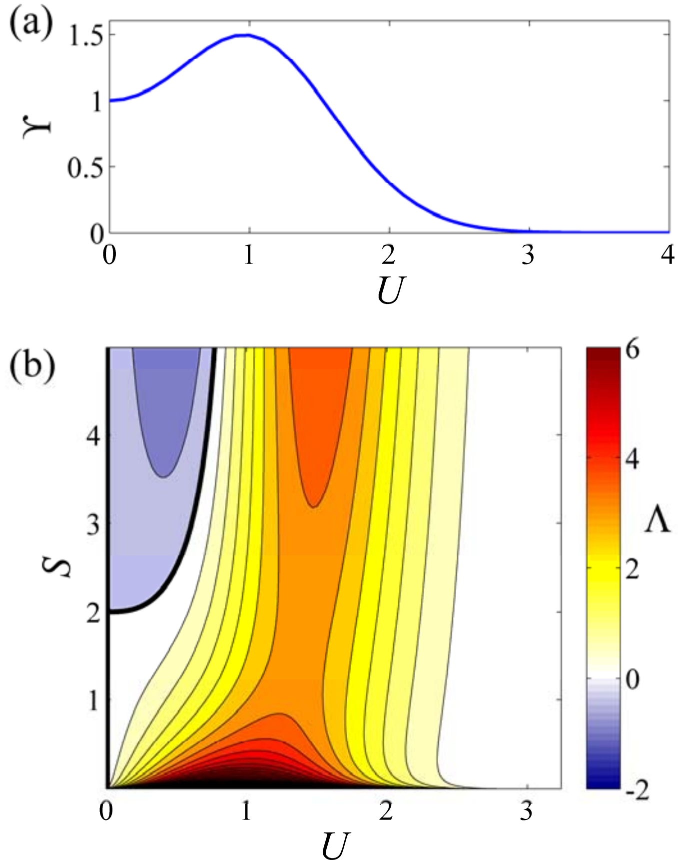

Figure 2.

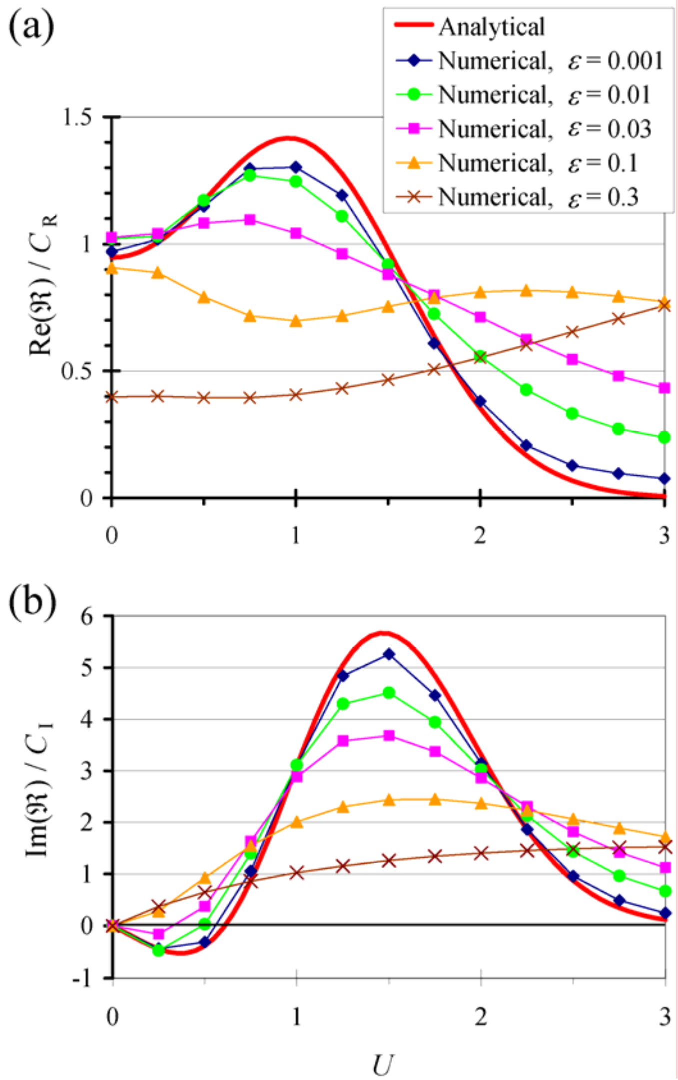
(a)
Analytical
Numerical, $\varepsilon = 0.001$
Numerical, $\varepsilon = 0.01$
Numerical, $\varepsilon = 0.03$
Numerical, $\varepsilon = 0.1$
Numerical, $\varepsilon = 0.3$
Re($\Re$) / C_R
(b)
Im($\Re$) / C_I
U